

Radiofrequency polarization effects in low-field electron paramagnetic resonance

C. J. Wedge, Christopher T. Rodgers, Stuart A. Norman, Neville Baker,
Kiminori Maeda, Kevin B. Henbest, C. R. Timmel and P. J. Hore

SUPPORTING INFORMATION

S1. Rotating frame approximation

Since the earliest days of NMR, the rotating frame transformation has been used to simplify the calculation and discussion of spin dynamics by removing from the spin Hamiltonian the time-dependence associated with the applied oscillating magnetic field. Switching from the laboratory co-ordinate system to one that rotates about the static magnetic field at the frequency of the orthogonal oscillating field gives a time-independent Hamiltonian (see Ref¹ for details).

In high-field magnetic resonance spectroscopy, the oscillating fields are typically linearly polarized (LP). We may write a LP radiofrequency field of root-mean-square strength B_1 and frequency ω_{RF} as the superposition of two notional circularly polarized (CP) fields

$$\mathbf{B}_{\text{LP}}(t) = \mathbf{i}\sqrt{2}B_1 \cos \omega_{\text{RF}}t = \mathbf{B}_{\text{CP}+}(t) + \mathbf{B}_{\text{CP}-}(t)$$

where

$$\mathbf{B}_{\text{CP}\pm}(t) = \mathbf{i}\sqrt{\frac{1}{2}}B_1 \cos \omega_{\text{RF}}t \pm \mathbf{j}\sqrt{\frac{1}{2}}B_1 \sin \omega_{\text{RF}}t$$

and \mathbf{i} and \mathbf{j} are the unit vectors along the x - and y -axes respectively. The rotating frame transformation cannot in general eliminate the time-dependence of the Hamiltonian for a spin system subject to $\mathbf{B}_{LP}(t)$. However, when ω_{RF} is close to the Larmor frequency, the $\mathbf{B}_{CP+}(t)$ component is almost on resonance with the spins while the $\mathbf{B}_{CP-}(t)$ component is $\sim 2\omega_{RF}$ off resonance. In high field NMR and EPR, this resonance offset is large enough that it is an excellent approximation to neglect the effect of $\mathbf{B}_{CP-}(t)$. The rotating frame transformation then removes the time-dependence of $\mathbf{B}_{CP+}(t)$ allowing the spin dynamics to be calculated using a time-independent Hamiltonian, an approach known as the “rotating frame approximation”²⁻⁷.

The situation is more complex when the applied static field (\mathbf{B}_0) is not much stronger than the other magnetic interactions experienced by the spins, as in the experiments reported here. Then, the effect of $\mathbf{B}_{CP-}(t)$ can no longer be ignored, and the rotating frame approximation is no longer valid. The approximation is also inapplicable when, as in some of the experiments reported here, the static and time-dependent (LP or CP) fields are not mutually orthogonal.

S.2 Experimental data for [Py- $d_{10}^{\bullet+}$ 1,3-DCB $^{\bullet-}$]

Figures 1 and 2 of the main paper presented the optically detected low-field EPR spectra of [Py- $h_{10}^{\bullet+}$ 1,3-DCB $^{\bullet-}$] (effective hyperfine coupling, $\langle a \rangle = 40.6$ MHz) and [Chr- $d_{12}^{\bullet+}$ 1,4-DCB $^{\bullet-}$] ($\langle a \rangle = 13.9$ MHz). Having $\langle a \rangle = 30.0$ MHz, [Py- $d_{10}^{\bullet+}$ 1,3-DCB $^{\bullet-}$] serves as an intermediate case. As shown in Figure S1, the principal spectral features observed for [Py- $h_{10}^{\bullet+}$ 1,3-DCB $^{\bullet-}$] and [Chr- $d_{12}^{\bullet+}$ 1,4-DCB $^{\bullet-}$] are also present for [Py- $d_{10}^{\bullet+}$ 1,3-DCB $^{\bullet-}$]. As might be expected, the [Py- $d_{10}^{\bullet+}$ 1,3-DCB $^{\bullet-}$] spectra resemble those of [Py- $h_{10}^{\bullet+}$ 1,3-DCB $^{\bullet-}$] more closely than of [Chr- $d_{12}^{\bullet+}$ 1,4-DCB $^{\bullet-}$], because of the common anion radical.

Still, many of the features observed for $[\text{Py-}d_{10}^{*\pm} \text{1,3-DCB}^{\bullet-}]$ are intermediate between those of $[\text{Py-}h_{10}^{*\pm} \text{1,3-DCB}^{\bullet-}]$ and $[\text{Chr-}d_{12}^{*\pm} \text{1,4-DCB}^{\bullet-}]$.

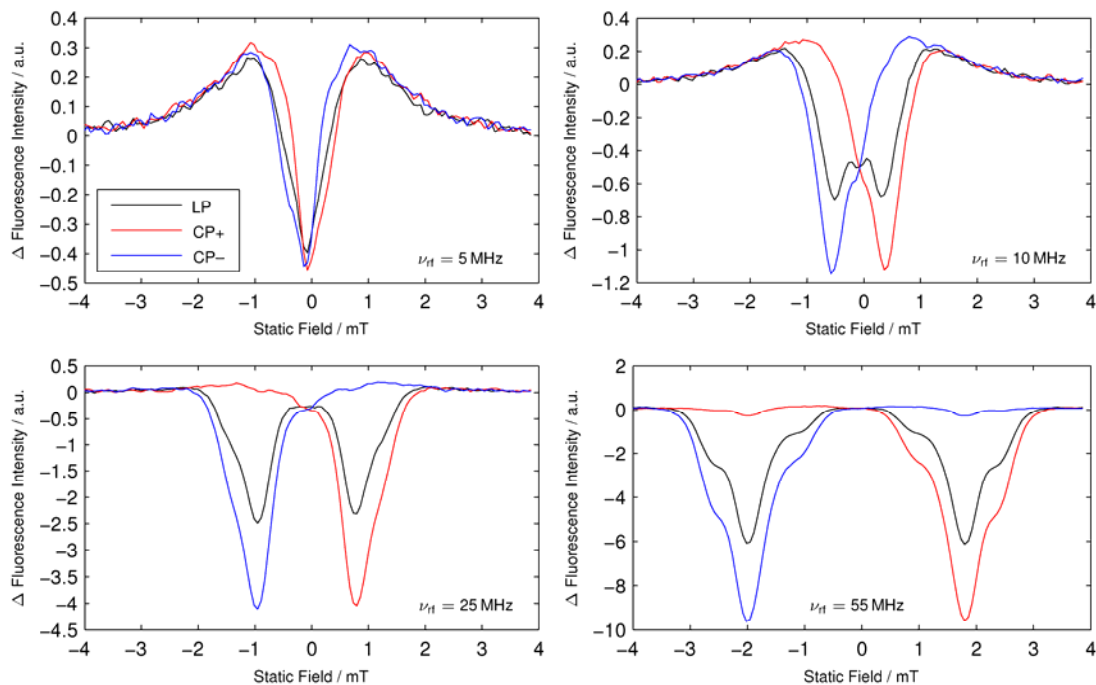


Figure S1. Experimental data for $[\text{Py-}d_{10}^{*\pm} \text{1,3-DCB}^{\bullet-}]$. $\theta_{\text{RF}} = 90^\circ$.

S.3 Spectral simulation using a static field approach

For sufficiently low frequencies, the RF field (\mathbf{B}_1) is effectively constant during the lifetime of the radical pair so that one can no longer expect true resonant features in the spectra. It has been shown previously that in this low-frequency limit an LP field may be described as an additional static field.^{8,9} The spectra can then be simulated by considering the total static field as $\mathbf{B}_{\text{eff}} = \mathbf{B}_0 + \mathbf{B}_1$ with the magnitude of \mathbf{B}_1 averaged over a suitable number of values of the initial RF phase, γ . Using such an approach it is possible to account for the observed dependence of the spectra on the angle between \mathbf{B}_0 and \mathbf{B}_1 as long as the RF period exceeds the lifetime of the radical pair, as exemplified by simulations of $[\text{Py-}d_{10}^{*\pm} \text{1,3-DCB}^{\bullet-}]$ with $B_1 = 300 \mu\text{T}$ and $k = 4 \times 10^7 \text{ s}^{-1}$ and $\nu_{\text{RF}} \approx 5 \text{ MHz}$.⁹

Here, we extend this approach to CP fields. Whereas in the LP case, \mathbf{B}_{eff} is the vector sum of the static field and a field \mathbf{B}_1 of varying magnitude but fixed direction, for a CP field, the magnitude of \mathbf{B}_1 is constant but its orientation with respect to the static field changes, see Figure S2. The angle between \mathbf{B}_0 and the xy -plane (in which the RF field is considered to rotate) is fixed for any given calculation, while the angle ϕ steps with the initial RF phase angle, γ . We define ψ as the angle between \mathbf{B}_0 and \mathbf{B}_1 , and as can be seen from the construction in Figure 2(b) we require only this angle and the magnitudes of the fields to find the resultant, \mathbf{B}_{eff} . The problem therefore simply reduces to that of determining ψ according to $\cos \psi = \cos \theta \cos \phi$, leading to the simple expression

$$B_{\text{eff}} = \left[(B_0)^2 + (B_1^{\text{CP}})^2 + 2B_0B_1^{\text{CP}} \cos \theta \cos \phi \right]^{\frac{1}{2}}$$

As would be expected if we set $\phi = 0$ as in the LP case this reduces to,

$$B_{\text{eff}} = \left[(B_0)^2 + (B_1^{\text{LP}})^2 + 2B_0B_1^{\text{LP}} \cos \theta \right]^{\frac{1}{2}}$$

Owing to the method of field generation used in our experiments the maximum RF amplitudes in the LP and CP cases are not equal. Taking B_1 as the amplitude of the CP radiofrequency field, we let $\phi = \gamma$ in the CP case and $B_1^{\text{LP}} = B_1 \sqrt{2} \cos \gamma$ in the LP case to obtain

$$\begin{aligned} B_{\text{eff}} &= \left[(B_0)^2 + (B_1)^2 + 2B_0B_1 \cos \theta \cos \gamma \right]^{\frac{1}{2}} && \text{CP fields} \\ B_{\text{eff}} &= \left[(B_0)^2 + 2(B_1)^2 \cos^2 \gamma + 2\sqrt{2}B_0B_1 \cos \theta \cos \gamma \right]^{\frac{1}{2}} && \text{LP fields} \end{aligned}$$

In both cases the yield of the reaction product should be averaged over a sufficient number of values of γ ($0 \leq \gamma \leq \pi$).

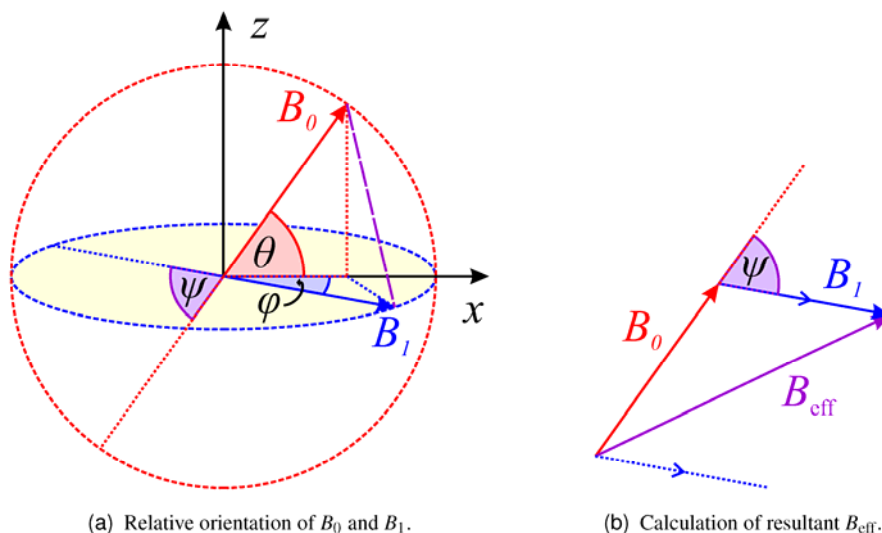


Figure S2. Angle definitions used when considering the 5 MHz low-field EPR spectra as a static field effect. The B_0 and B_1 fields are shown in red and blue respectively, with the dashed lines showing the ranges of variation. The B_0 field lies in the xz -plane at an angle θ to the x -axis; in the CP case the B_1 field rotates in the xy -plane making an angle ϕ to the x -axis; ψ is the angle between the two fields.

Simulations for $[\text{Py-}h_{10}^{*+} 1,3\text{-DCB}^{*-}]$ are shown in Figure S3, for $B_1 = 100 \mu\text{T}$.

Although not a perfect match to the experimental results (reproduced here from Figure 4 of the main paper for comparison), the major differences between the LP and CP spectra are reproduced, the orientation dependence being much more pronounced in the former case. The simulations are not expected to reproduce the slight asymmetry of the CP data which is clearly a resonant effect that cannot be accounted for in this ‘static’ approach.

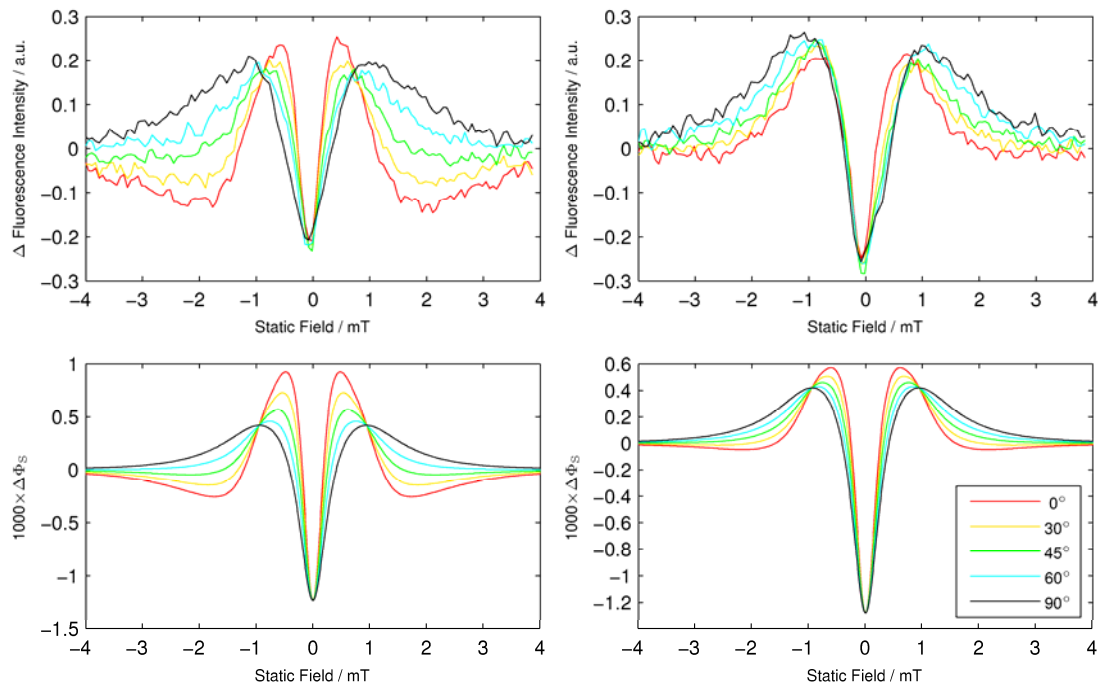


Figure S3. Experimental data for $[\text{Py-}h_{10}^{\bullet+} \text{1,3-DCB}^{\bullet-}]$ for $\nu_{\text{RF}} = 5$ MHz (top) and the corresponding simulations using the static field shift approach (bottom), showing the difference between LP (left) and CP+ (right) polarizations. $k = 4 \times 10^7 \text{ s}^{-1}$.

S.4 Importance of small hyperfine interactions

Figure S4 illustrates, for the case of $[\text{Py-}h_{10}^{\bullet+} \text{1,3-DCB}^{\bullet-}]$, that the quality of the simulated (γ -COMPUTE) low-field EPR spectra depends on the number of hyperfine couplings included. The spectra on the left were computed including just one set of equivalent protons in each radical (4×12.3 MHz for $\text{Py-}h_{10}^{\bullet+}$ and 2×23.2 MHz for $\text{1,3-DCB}^{\bullet-}$). Those on the right were simulated using two further sets of nuclei in each radical (4×5.94 MHz for $\text{Py-}h_{10}^{\bullet+}$ and 1×3.19 MHz for $\text{1,3-DCB}^{\bullet-}$). In connection with Figure 1 in the main paper we mentioned that the simulations tend to overestimate the negative OMFE component at zero static field in the low-frequency spectra. It is clear from Figure S4 that this feature is less pronounced (and hence a closer match to the experimental data) when the five extra hyperfine couplings are included. This is by no means an obvious result at all as the effective hyperfine couplings between the simulations in right and left panel correspond to 38.6 MHz and 40.1, respectively, that is just a 5% difference, yet the simulations are clearly a much better match illustrating impressively the importance that small hyperfine couplings

play in the appearance of the spectra. Similar effects are observed at 10 MHz when, again, inclusion of the smaller hyperfine couplings improves the prediction of the spectral shape at low static fields. Finally, the 55 MHz case (bottom panels) fulfills all high-field expectations, namely that the simulations are very similar for both sets of hyperfine couplings as the additional, small hyperfine couplings do not contribute significantly to the line broadening of the Zeeman resonance.

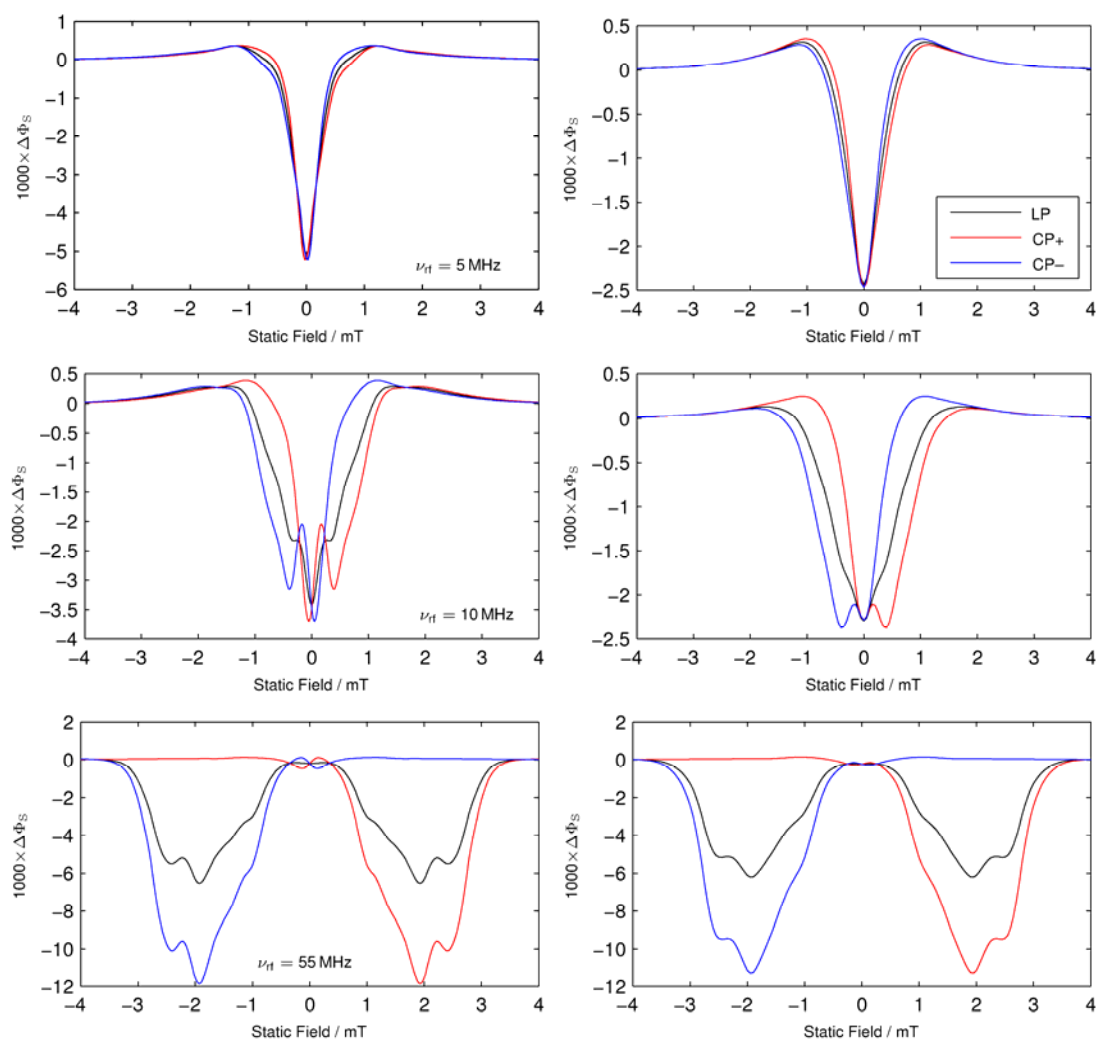


Figure S4. Simulations for $[\text{Py-}h_{10}^{*\text{+}} \text{1,3-DCB}^{*\text{-}}]$ using 2 groups of equivalent nuclei (left) and 4 groups of equivalent nuclei (right). $\theta_{\text{RF}} = 90^\circ$. $k = 4 \times 10^7 \text{ s}^{-1}$.

References

- 1 M. H. Levitt, *Spin Dynamics*, Wiley, Chichester, 2008.
- 2 I. I. Rabi, N. F. Ramsey and J. Schwinger, *Rev. Mod. Phys.*, 1954, **26**, 167-171.
- 3 R. K. Wangsness and F. Bloch, *Phys. Rev.*, 1954, **89**, 728-739.
- 4 F. Bloch, *Phys. Rev.*, 1946, **70**, 460-474.
- 5 F. Bloch and A. Siegert, *Phys. Rev.*, 1940, **57**, 522-527.
- 6 J. Schwinger, *Phys. Rev.*, 1937, **51**, 648-651.
- 7 F. Bloch, *Phys. Rev.*, 1956, **102**, 104-135.
- 8 C. T. Rodgers, D. Phil. thesis, University of Oxford, 2007.
- 9 C. T. Rodgers, K. B. Henbest, P. Kukura, C. R. Timmel and P. J. Hore, *J. Phys. Chem. A*, 2005, **109**, 5035-5041.